5 Spectacular explosions

Supernovae- super new (stars)- $L \sim 10^{42}$erg/s on tens of days times scale. Divided to Type II- showing H lines, and Type I- no H lines. Within I: Type Ia- showing Si lines, Ib/c- no Si lines, Ib with He lines, Ic no (or weak) He lines. As discussed in § 3.4, Type II and Ib/c are believed to result from core collapse (CC) of massive stars (with Ib/c being stripped of their H envelope), while type Ia's are believed to be produced by the accretion induced collapse of WDs. We will discuss here CC SNe. The association of SNe with CC of massive stars was motivated first by indirect evidence: (i) The gravitational energy released in CC is sufficient to power the SN (Baade & Zwicky 1934); (ii) Elemental abundances in SN expanding ejecta and in SN remnants (SNR) may be explained by explosive nucleosynthesis in the mantle of massive stars; (iii) Neutron stars (NSs) found at the centers of SNRs. Direct evidence: Detection of ν's from SN1987A, and association of SN1987A with a BSG in the LMC.

5.1 Preliminaries: Hydrodynamics

Consider the velocity field $\mathbf{v}(\mathbf{x},t)$ of a non-relativistic "ideal fluid" at LTE (Local Thermal Equilibrium): its state at every point is determined by two thermodynamic parameters, say p and ρ, with momentum flux tensor at its local rest frame given by $\Pi_{ij} = p\delta_{ij}$ (neglecting diffusive contributions from gradients). We assume that the time scale for variations in the flow are long enough to allow LTE, and that the length scales are large enough to allow neglecting additional terms in Π_{ij}. Conservation of mass, $d(\int_V dV\rho)/dt = \int_V d^3V\partial_t\rho = \int_{\partial V} d^2\mathbf{S}.(\rho\mathbf{v}) = \int_V d^3V\nabla(\rho\mathbf{v})$ gives the continuity equation,

$$(\partial_t + \mathbf{v}.\nabla)\rho + \rho\nabla\mathbf{v} = 0. \tag{143}$$

Conservation of momentum, $\int_V d^3V\partial_t(\rho v_i) = \int_{\partial V} dS_j\Pi_{ij}$ with $\Pi_{ij} = p\delta_{ij} + \rho v_i v_j$ gives Euler's eq.

$$(\partial_t + \mathbf{v}.\nabla)\mathbf{v} = -\frac{1}{\rho}\nabla p. \tag{144}$$

Note, $(\partial_t + \mathbf{v}.\nabla)$ is the gradient along a fluid element trajectory: For any function $f(\mathbf{x},t)$, df along a fluid element trajectory is $df = \partial_t f dt + \nabla f.d\mathbf{x} = \partial_t f dt + \nabla f.\mathbf{v}dt = dt(\partial_t + \mathbf{v}.\nabla)f$. It is thus common to use $d/dt \equiv (\partial_t + \mathbf{v}.\nabla)$. Since the fluid is always at LTE the entropy of fluid elements is conserved, i.e. the flow is adiabatic, i.e.

$$ds/dt \equiv (\partial_t + \mathbf{v}.\nabla)s = 0. \tag{145}$$

The 5 eqs., eqs. (143-145), determine the evolution of the 5 variables, $\{\mathbf{v}, \rho, p\}$. The relation between s and $\{p, \rho\}$ is determined by the equation of state (eos) of the fluid.

Using eqs. (143-145) (and $Tds = d\epsilon + pd(1/\rho)$) it is straightforward to show that

$$\partial_t \left(\frac{1}{2}\rho v^2 + \rho\epsilon \right) + \nabla \left[\left(\frac{1}{2}v^2 + h \right) \rho \mathbf{v} \right] = 0, \tag{146}$$

where ϵ is the internal energy (per mass) and $h = \epsilon + \frac{p}{\rho}$ the enthalpy.

Sound Waves. Consider a small perturbation to a uniform, static fluid: $\rho = \rho_0 + \delta\rho$, $p = p_0 + \delta p$. Linearizing eqs. (143-145), noting that v is first order, we have

$$\partial_t \delta\rho + \rho_0 \nabla \mathbf{v} = 0, \quad \partial_t \mathbf{v} + \rho_0^{-1} \nabla \delta p = 0, \quad \partial_t \delta s = 0. \tag{147}$$

Fourier transforming, $f(\mathbf{x}, t) \propto \exp(\mathbf{k}.\mathbf{x} - \omega t)$,

$$\omega\delta\rho = \rho_0 \mathbf{k}.\mathbf{v}, \quad \omega\mathbf{v} = \rho_0^{-1}\mathbf{k}\delta p, \quad \omega\delta s = 0. \tag{148}$$

A general perturbation, with given $\mathbf{k}$, may be decomposed into 3 types of perturbations: (i) Entropy perturbation: $\{\delta s \neq 0, \delta p = 0, \mathbf{v} = 0, \omega = 0\}$; (ii) Adiabatic incompressible ($\nabla \mathbf{v} = 0$ i.e. $\mathbf{k} \perp \mathbf{v}$) perturbations: $\{\delta s = 0, \delta p = 0, \mathbf{k}.\mathbf{v} = 0, \omega = 0\}$; (iii) Adiabatic compressible perturbations $\{\delta s = 0, \delta p \neq 0, \mathbf{k} \parallel \mathbf{v}\}$. It is straight forward to obtain the dispersion relation for (iii),

$$\frac{\omega^2}{k^2} = c_s^2, \quad c_s^2 \equiv \left(\frac{\partial p}{\partial \rho} \right)_s. \tag{149}$$

Small pressure perturbations propagate with (group & phase) velocity c_s, the "speed of sound". For these perturbations, $\mathbf{v} = \pm(\delta\rho/\rho_0)c_s\hat{\mathbf{k}}$, implying that the linear analysis applies for $v/c_s \ll 1$. For ideal gas eos, $c_s^2 = \gamma p/\rho$ so that the speed of sound is comparable to the thermal velocity of the particles (recall $p/\rho = T/\mu$).

Shock Waves. It is possible to show that not only small perturbation propagate at c_s, but rather that any information can not propagate with respect to the fluid faster than c_s. What happens, then, when a piston propagates at velocity v into a uniform fluid with some c_s? When $v > c_s$ there is no way for the information to propagate ahead of the piston, i.e. there is no way to inform the fluid that it should move before the piston "hits" it. In this case, a discontinuity in the flow forms, which propagates ahead of the piston at a velocity larger than c_s. That is, some transition layer is formed within which the characteristic time and length scales for changes

in the fluid properties are not sufficient to keep LTE. Assuming that the thickness of this layer is small compared to the characteristic length scales of the flow in which we are interested, we may consider it to be a discontinuity.

Across the discontinuity, the flux of mass, momentum and energy must be conserved (the entropy may change since the fluid is not in LTE within the transition layer). Consider thus a planar discontinuity at rest (we can always examine a small part of the discontinuity layers which is approximately planar, and choose our rest frame to coincide with that of the discontinuity). Denoting by $[f]$ the difference between the values of any property of the flow at the two sides of the discontinuity, we may write the conservation of mass, momentum and energy as (see eqs. 143-145)

$$[\rho v_x] = 0, \quad [p + \rho v_x^2] = [\rho v_x v_y] = [\rho v_x v_z] = 0, \quad [\rho v_x (\frac{1}{2} v^2 + h)] = 0, \quad (150)$$

where we have chose the x direction to be perpendicular to the discontinuity plane.

There are 2 types of discontinuities: (i) A tangential discontinuity in which there is no mass flux across the discontinuity (i.e. it moves with the fluid), $\rho v_x = 0$, accros which the pressure is continuous, $[p] = 0$, but the tangential velocity may is discontinuous, e.g. $[v_y] \neq 0$; (ii) A shock wave, where there is mass flux, $j = \rho v_x \neq 0$ (i.e. the discontinuity propagates through the fluid), and there is no tangential velocity jump, $[v_y] = [v_z] = 0$.

For the shock wave, it is straightforward to obtain

$$j^2 = -\frac{p_2 - p_1}{V_2 - V_1}, \quad v_1 - v_2 = \sqrt{(V_1 - V_2)(p_2 - p_1)}, \quad (151)$$

and

$$h_1 - h_2 + \frac{1}{2}(V_1 - V_2)(p_2 + p_1) = 0, \quad (152)$$

where the indices 1 and 2 denote values on the two sides of the discontinuity, and $V \equiv 1/\rho$. We choose the velocities to be positive and the index 1 to denote the values of flow variables in the region where the fluid is approaching the discontinuity. The shock velocity and the post-shock fluid velocity in the frame where the pre-shock fluid is at rest are v_1 and $v_1 - v_2$ respectively.

Eq. (152) gives a relation between p_2 and V_2 for any given p_1 and V_1 (recall $h(p, V)$). This relation, say $p_2(V_2; p_1, V_1)$, is called the Rankine-Hougoniot "shock adiabatic". At the the discontinuity, the thermodynamic parameters "jump" from $\{p_1, V_1\}$ to a point $\{p_2, V_2\}$ on the shock adiabatic. Eqs. (151-152) are also called the "shock jump conditions". Since eqs. (151) give v_1 and v_2 as functions of p_2 and V_2 (for given $\{p_1, V_1\}$), the "jump"

is determined by a single parameter (p_2, V_2, v_1 or v_2). The entropy must increase across the shock, $s_2 > s_1$. for all known eos this condition is satisfied iff $p_2 > p_1$, which implies also $v_1 > v_2$ (deceleration) and $\rho_2 > \rho_1$ (compression). Thus, at the shock, the fluid is compressed and part of its kinetic energy is converted to thermal energy. It is also possible to show that $v_1 > c_{s1}$ and $v_2 < c_{s2}$. $M_1 \equiv v_1/c_{s1}$ is called the "shock Mach number".

For ideal gas eos, $h = \gamma p/(\gamma - 1)\rho$, in the limit $M_1 \equiv v_1/c_1 \gg 1$,

$$\frac{p_2}{p_1} = \frac{2\gamma}{\gamma+1} M_1^2, \quad \frac{v_1}{v_2} = \frac{\rho_2}{\rho_1} = \frac{\gamma+1}{\gamma-1}, \quad v_1 - v_2 = \frac{2}{\gamma+1} v_1. \tag{153}$$

The post-shock speed of sound is

$$c_{s2} = \frac{\sqrt{2\gamma(\gamma-1)}}{\gamma+1} v_1. \tag{154}$$

5.2 Core collapse SNe

Recall: stellar core evolution tracks, stars with $8 \leq M/M_\odot \leq 70$ develop cores with $M_{\rm core} > M_{\rm ch}$ and do not enter the pair-instability region, move to Fe dissociation. At the relevant $T \sim 0.7$ MeV, the core radius is $R_c \sim GM\mu/T \sim 10^8$ cm and the core density is $\rho \sim 10^{8.5}{\rm g/cm}^3$. The dissociation of $^{56}_{26}$Fe to $13\alpha + 4n$ requires 124 MeV. Leads to $\gamma < 4/3$, instability and collapse. The characteristic collapse time is

$$t_{\rm ff} \sim \frac{1}{\sqrt{G\rho}} \sim 0.1 \rho_9^{-1/2} {\rm s}, \tag{155}$$

where $\rho = 10^9 \rho_9 {\rm g/cm}^3$. At the onset of the collapse, $t_{\rm ff} \sim R/c_s$. However, as the collapse proceeds, $t_{\rm ff} \ll R/c_s$, compare e.g. $t_{\rm ff} \sim \rho^{-1/2}$ with $c_s \propto \rho^{(\gamma-1)/2}$ and $R/c_s \propto \rho^{-(3\gamma-1)/6}$ for adiabatic compression.

Neutronization. Inverse β-decay, $e^- + p \to n + \nu_e$, converts p's to n's. The threshold energy is $(m_n - m_p)c^2 = 1.3$ MeV. At sufficiently high density, the Fermi energy of the electrons may be high enough to prevent the decay $n \to p + e + \bar{\nu}$. Recall that for $T = 0$ we have $p_{f,e} = (3\pi^2)^{1/3} \hbar n_e^{1/3}$, i.e.

$$p_{f,e} c = 5 (Y_e \rho_9)^{1/3} {\rm MeV}, \tag{156}$$

where $Y_e = n_e/n_b$. As the collapse proceeds, neutronization proceeds through $e^- + (Z, A) \to (Z-1, A) + \nu_e$.

Neutrino trapping. Neutrinos are scattered by e^- and nuclei. Estimating $\sigma \sim G_F^2 A^2 E_\nu^2$ (for coherent nucleus scattering) and $E_\nu = p_{f,e} c$

we have $\sigma \sim 10^{-43} A^2 \rho_9^{2/3} \mathrm{cm}^2$ and $\lambda_\nu \sim 10^{10} A^{-1} \rho_9^{-5/3}$ cm. The neutrinos become trapped when $t_{\rm ff} < (R/\lambda_\nu)(R/c)$, i.e. for

$$\rho_{\rm trap.} \sim 3 \times 10^{11} (M/M_\odot)^{-4/9} \mathrm{g/cm}^3. \tag{157}$$

At early stages of the collapse, $\rho < \rho_{\rm trap.}$, ν_e's escape and neutronization proceeds via the inverse β-decay. At higher densities, neutrinos are trapped and the resulting high Fermi energy of the neutrinos prevents neutronization. This keeps Y_e high and heavy nuclei present till nuclear densities are reached.

"Core bounce". When nuclear densities are reached, $\rho_{\rm nuc.} \sim 10^{14.5} \mathrm{g/cm}^3$, the nucleon contribution to the pressure becomes large, the eos "stiffens", and the collapse is halted. This occurs at a radius of

$$R_{\rm bounce} \sim 10^6 (M/M_\odot)^{1/3} \mathrm{cm}. \tag{158}$$

The gravitational energy released is

$$E_G \sim \frac{GM^2}{R} = 10^{53.5} \frac{(M/M_\odot)^2}{R/10\mathrm{km}} \mathrm{erg}. \tag{159}$$

This energy leaks out from the core by the diffusion of neutrinos, on a time scale of ~ 3 s, giving $L_\nu \sim 10^{53} \mathrm{erg/s}$. The characteristic ν energy is 10's of MeV (energy is carried by photons, pairs, ν's).

Envelope ejection? Since the collapse of the outer shells is faster than the speed of sound, the core collapse halt leads to the formation of a shock wave that propagates outwards and decelerates the in-falling envelope. In model calculations, the shock is stalled by the inflow, and eventually collapses. The envelope is not ejected and falls back onto the nuclear density core, which can not support it (see § 5.4) and collapses to a BH. As mentioned above, it is believed that the collapse of the core leads to SN explosion. Thus, it is assumed that somehow the shock is "revived" and expels the envelope. Current research- focuses on 3D effects (deviations from spherical explosions). We first discuss the observational consequences of such expulsion. A discussion of the fate of the collapsed core that reached nuclear density will be given later.

The energy required to expel the envelope is $\sim 10^{51}$ erg. Suppose such energy is damped into the envelope. The thermal energy density will be dominated by radiation, with

$$T_0 \sim 200 \frac{E_{51}^{1/4}}{R_{*,13}^{3/4}} \mathrm{\ eV}, \tag{160}$$

where $E = 10^{52}E_{51}$ erg, and the stellar radius is $R_* = 10^{13}R_{*,13}$ cm. Note that the thermal energy carried by the particles is only $\sim 10^{48}$ erg. The shock expanding in the envelope is thus mediated by radiation. The characteristic expansion velocity is

$$v \simeq 10^9 \frac{E_{51}^{1/2}}{(M/M_\odot)^{1/2}} \mathrm{cm/s}. \tag{161}$$

At the early stages of the expansion, the photon diffusion time, $t_D = R^2/\lambda c \approx R^2\kappa\rho/c \approx \kappa M/4Rc \approx 6 \times 10^8 (M/M_\odot)R_{13}^{-1}$ s (assuming electron scattering opacity and full ionization), is larger than the expansion time, $t_d = R/v \approx 10^4 R_{13}(M/M_\odot)^{1/2}E_{51}^{-1/2}$ s. As long as $t_D \gg t_d$ we may approximate the expansion as adiabatic, for which $T \propto R^{-1}$ and $E_{\rm rad} \propto R^3T^4 \propto R^{-1}$, and the luminosity $L = E_{\rm rad}/t_D \propto R^0$. Thus, we expect constant bolometric luminosity,

$$L \approx \frac{E}{t_D(R = R_*)} \approx 2 \times 10^{42} \frac{E_{51}R_{*,13}}{M/M_\odot} \mathrm{erg/s}, \tag{162}$$

up to the time at which $t_D = t_d$, i.e. up to

$$R \approx 2.5 \times 10^{15} E_{51}^{1/2}(M/M_\odot)^{1/2}, \quad t \approx 2.5 \times 10^6 E_{51}^{-1/4}(M/M_\odot)^{3/4}\mathrm{s}. \tag{163}$$

At this time the temperature is

$$T \approx 1 \frac{R_{*,13}^{1/4}}{E_{51}^{1/4}(M/M_\odot)^{1/2}} \mathrm{eV}, \tag{164}$$

the radiation escapes, and at later times L decays exponentially.

Explosive nucleosynthesis, radioactive decay. As mentioned in § 4, cosmological nucelosynthesis produces D, He, and traces of Li, Be. As explained in § 3.4.1, heavier nuclei from C to Ca are produced by fusion in stars. Fe group nuclei approximately in 0.1 MeV NSE, consistent with explosive synthesis in SN shocks. Mention s and r processes: Slow (s) process-neutron capture up to β-decay; Rapid (r) process- rapid neutron capture in high neutron flux environment, leading to neutron rich isotopes. Radioactive nuclei produced in the explosion decay and may contribute to the SN light emission: ^{56}Ni to ^{56}Co at 6.1 d and 1.7 MeV, ^{56}Co to ^{56}Fe at 77.1 d and 3.8 MeV, giving $E/M \simeq 10^{17}\mathrm{erg/g} = 2 \times 10^{50}\mathrm{erg/M_\odot}$. Production of UV/O emission requires absorption of the gamma-rays and their conversion to heat in the expanding envelope.

5.3 Supernova remnants (SNRs): Thermal emission

The SN ejecta expands into the ISM at a velocity $v \sim 10^4$km/s which far exceeds the ISM $c_s \sim 10$km/s ($T \sim 1$ eV). This implies that the ejecta drives a strong shock, $v_1 = (\gamma+1)v/2$ (see eq. 153) and $M_1 = v_1/c_{s1} \gg 1$, into the ISM. Since the post shock speed of sound and fluid velocity are comparable (compare $v_1 - v_2$ and c_{s2} in eqs. 153, 154), the total energy carried by the shocked ISM is comparable to $M_S v^2$, where M_S is the mass of the shock ISM. When this mass becomes comparable to the mass of the ejecta, most of the kinetic energy stored in the ejecta is transferred to the shock ISM. As the shock continues to expand and mass of shocked gas M_S increases, the shock must decelerate. Conservation of energy implies $E \sim M_S \dot{R}^2$ where R is the shock radius. For uniform density ISM, $M_S \propto R^3$ and $\dot{R} \propto R^{-3/2}$. The deceleration radius may be estimated requiring M_S to equal the ejecta mass M,

$$R_{\rm dec} \sim \left(\frac{M}{4\pi n m_p/3}\right)^{1/3} = 6.5{\times}10^{18}\left(\frac{M/M_\odot}{n_0}\right)^{1/3}{\rm cm} = 2.1\left(\frac{M/M_\odot}{n_0}\right)^{1/3}{\rm pc}, \tag{165}$$

where $n = 10^0 n_0 {\rm cm}^{-3}$ is the ISM density, and the deceleration time is

$$t_{\rm dec} \sim \frac{R_{\rm dec}}{v} = 210\frac{(M/M_\odot)^{5/6}}{n_0^{1/3}E_{51}^{1/2}}{\rm yr}. \tag{166}$$

For $R \gg R_{\rm dec}$, we have $M_S \gg M$ and a shock radius which is much larger than the characteristic size of the exploding object. It is reasonable to assume that at this stage the flow is no longer dependent on the exact details of the initial conditions, i.e. of the size and mass of the region in which the energy is initially deposited and of the initial spatial distribution of the fluid properties within this region. If this is the case, the flow should be completely determined by the explosion energy E and by the density and pressure of the ISM into which the shock expands, $\rho_0 = n_0 m_p$ and p_0. For a strong shock, $p_2 \gg p_1 = p_0$, the flow is also independent of p_0. The flow is determined by the hydrodynamic eqs. (143-145) with boundary conditions at the shock front given by the shock jump conditions. For an ideal gas eos, and as long as the shock is strong, these boundary conditions are given by eqs. (153,154).

The hydrodynamic eqs. contain no dimensional parameters. For an ideal gas, the eos, $e = p/(\gamma_1)\rho$, does not contain any dimensional parameters either. The flow fields, p, ρ and v, are functions of $\{E, \rho_0, r, t, \gamma\}$, and that R is a function of $\{E, \rho_0, t, \gamma\}$. The dimensions of any variable

f may be considered to be a 3-dimensional vector $\{\alpha_L, \alpha_M, \alpha_T\}$ such that $[f] = L^{\alpha_L} M^{\alpha_M} T^{\alpha_T}$. R is determined by 3 dimensional parameters with independent dimensions (i.e., with independent dimension vectors), $\{E, \rho_0, t\}$. Since the dimensions of these parameters are independent, there is only one product of powers of them which has the dimensions of length, $(Et^2/\rho_0)^{1/5}$, and there is no product of powers of these parameters which is dimensionless. This implies that R must be of the form

$$R = \zeta(\gamma) \left(\frac{E}{\rho_0} t^2\right)^{1/5} = 2.9\zeta(\gamma) \left(\frac{E_{51}}{n_0}\right)^{1/5} t_{10}^{2/5} \mathrm{pc}, \tag{167}$$

where $t = 10^{10} t_{10}$s, 10^{10}s $\simeq$ 300 yr. Note that this satisfies the energy conservation result $\dot{R} \propto R^{-3/2}$. $\zeta(\gamma)$ is a dimensionless function, with values close to unity. The post shock density is enhance by a factor $(\gamma+1)/(\gamma-1) \sim 4$, so that most of the shocked ISM is compressed into a shell of thickness $\Delta/R \sim (\gamma-1)/3(\gamma+1) < 0.1$. The temperature of the post shock plasma is (see eq. 154)

$$T \approx \frac{2(\gamma-1)}{(\gamma+1)^2} \mu \dot{R}^2 \approx 10 \left(\frac{E_{51}}{n_0}\right)^{2/5} t_{10}^{-3/5} \mathrm{keV}. \tag{168}$$

We therefore expect thermal X-ray emitting shells of several pc radius on a time scale of thousand years following the SN explosion. The distribution of SNR radii should follow $N_{SNR}(< R) = \dot{N}_{SN} t(R) \propto R^{5/2}$, where $\dot{N}$ is the NS rate. Such remnants are observed both in the Milky Way and in the SMC/LMC, with properties consistent with those described above. In some cases, the remnants are associated with documented SNe, like SN1054 (exploded in 1054, remnant 1000 yrs old).

The remnant parameters $\{E, \rho_0, t\}$ may be inferred from the measured radius R, X-ray luminosity (dominated by Bremsstrahlung) and temperature (inferred from the spectrum). In most Galactic cases, the distance, and hence R, is not accurately known, leading to uncertainties in inferred parameters. Another uncertainty is due to the possibility that the electrons and ions are not in thermal equilibrium (see § 5.5).

5.4 Some comments on Neutron Stars (NSs)

As ν's escape the core becomes a (cold) NS. Assuming ideal degenerate cold neutron gas, the mass-radius relation is obtained in a manner similar to that for WDs, see eq. (46),

$$R_{NS} \approx 4.3 \frac{\hbar^2}{G m_p^{8/3}} M^{-1/3} = 12 (M/M_\odot)^{-1/3} \mathrm{km}. \tag{169}$$

The maximum mass is obtained when the degenerate neutrons become relativistic, see eq. (47),

$$M_{NS} < 3.5 \left(\frac{\hbar c}{G m_p^2}\right)^{3/2} m_p = 5.6 M_\odot. \tag{170}$$

These results are not accurate, since we neglected the strong interaction between neutrons at nuclear densities (and also GR corrections, $\Phi/c^2 = GM/R_{NS}c^2 \sim 0.1$). The eos at nuclear densities is not known and is a subject of current research, commonly used eos reduce the maximum mass to $\sim 3M_\odot$. It is hoped that NS $M-R$ relation measurements would help in constraining the eos (so far not accurate enough, see e.g. arXiv:1005.0811).

Evidence for the existence of NSs: Pulsars & X-ray binaries.

5.4.1 Pulsars

Pulsars were first detected in '68- radio sources emitting a periodic radio signal, with periods $\sim$ 1ms $< P <\sim$ 10 s ($\sim$ 2000 now known, see arXiv:1004.2730). Angular distribution (of the objects) implies Galactic sources. No luminous star identified to be associated. The period suggests an upper limit to the size, $R < cP \sim 300$ km. Estimating the minimum density for a gravitationally bound rotating/pulsating object from $t > 1/\sqrt{G\rho}$ we have

$$\rho > 10^{13} (P/1\text{ms})^{-2} \text{g/cm}^3. \tag{171}$$

The high density and small radius require a NS.

P is highly stable, measured for pulsars with 10-13 significant digits. P grows slowly with time, typically $P/\dot{P} \sim 10^{10}$ s. If the periodicity is due to NS rotation, the associated energy is $E_{\rm rot.} = \frac{1}{2} I\omega^2$, $\omega = 2\pi/P$. The exact value of the moment of inertia depends on the eos. Roughly,

$$E_{\rm rot.} = \frac{1}{2} I\omega^2 \simeq \frac{3}{10} MR^2\omega^2 = 2 \times 10^{50} (M/M_\odot) R_6^2 P_{-2}^{-2} \text{erg}, \tag{172}$$

where $R = 10^6 R_6$ cm and $P = 10^{-2} P_{-2}$ s. The growth of P implies rotational energy loss at a rate of

$$-\dot{E}_{\rm rot.} = -I\omega\dot{\omega} = 2E_{\rm rot.} \frac{\dot{P}}{P} = 2 \times 10^{40} (M/M_\odot) R_6^2 P_{-2}^{-2} \left(\frac{\dot{P}}{P}\right)_{-10} \frac{\text{erg}}{\text{s}}, \tag{173}$$

where $\dot{P}/P = 10^{-10} (\dot{P}/P)_{-10} \text{s}^{-1}$.

The Crab pulsar is located at the center of the Crab nebula- a SNR consistent with the SN documented to have exploded in 1054. The SNR shell is filled with radiation emitting plasma (radio to gamma-rays), the "nebula". The rate at which energy is inferred to be deposited in the nebula (to account for the emitted radiation) is $\dot{E} \sim 10^{39}$erg/s. The rotational energy loss implied for this pulsar, with $P_{-2} = 3.3$ and $(\dot{P}/P)_{-10} = 0.13$, is $-\dot{E}_{\rm rot.} \sim 10^{39}$erg/s, suggesting that the nebula is powered by the energy loss of the pulsar. An age estimate of $\sim P/\dot{P} \sim 10^3$ yr is consistent with SN1054.

It was speculated, before the discovery of pulsars, that NS may be born with strong magnetic fields, due to the amplification of the stellar magnetic field during collapse (the magnetic field at the surface of the Sun is $\sim$kG). A magnetized rotating NS would lose energy through emission of electromagnetic waves at a rate $\dot{E} = -2|\ddot{\mathbf{m}}|/3c^3$ where the magnetic dipole may be estimate as BR^3. In order to account for the energy loss, we need

$$B \sim c^{3/2}\dot{E}^{1/2}P^2R^{-3} = 10^{13}\dot{E}_{39}^{1/2}P_{-2}^2R_6^{-3}{\rm G}. \tag{174}$$

It is thus inferred that NS are highly magnetized.

5.4.2 X-ray pulsars and X-ray binaries

X-ray sources were detected in the early '60's. Angular distribution- suggesting Galactic sources. Many discovered to pulsate, $P \sim 1$ s. Many associated with optically identified stars, which are in a binary system (inferred from periodic Doppler shifts of their spectral lines) with an optically-invisible companion. The optically invisible companion may be a WD or NS. The short period implies $\rho > 10^7{\rm g/cm}^3$. Marginal for WD, and heating the WD surface to keV would "puff" it up to radii much larger, and densities much lower, than those of cold WDs. Hence, the companion is likely a NS.

The mass M_1 of the invisible companion may be inferred from the velocity and mass M_2 of the optically identified star. For circular orbits we have (see § 3.1)

$$f(M) \equiv \frac{(M_1 \sin i)^3}{(M_1+M_2)^2} = \frac{v_{\rm 1obs,max}^3 T}{2\pi G}, \tag{175}$$

where i is the orbit's inclination angle. Determining M_2 from the optical data, constraints on M_1 are implied with uncertainty largely due to uncertainty in i. For eclipsing X-ray binaries, $i = \pi/2$, the companion mass can be inferred rather accurately- see e.g. van der Meer et al. 2007 (A&A 473, 523), who give $M_1/M_\odot = \{1.1, 1.3, 1.3\} \pm 0.1$ for 3 "famous" binaries.

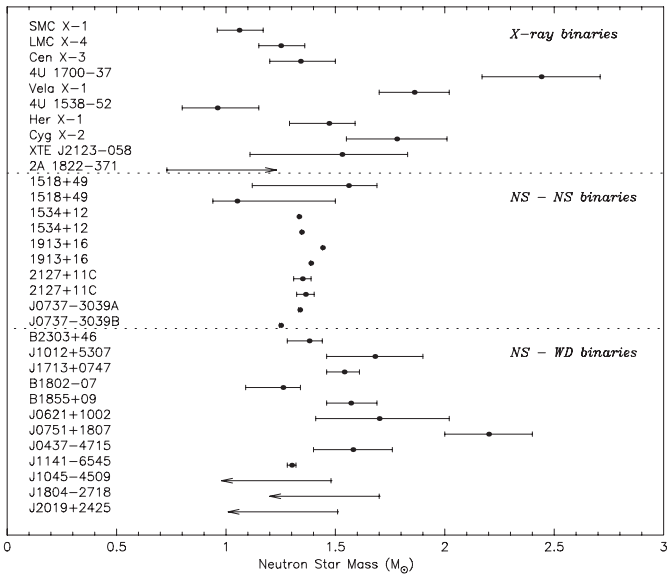

Figure 6: NS masses inferred from binary systems observations, van der Meer et al. 2007 (A&A 473, 523).

In some cases, where the inferred mass is larger than $3M_\odot$ (e.g. Cyg X-1 with $M_1/M_\odot > 3.4$), it is argued that the companion must be a black hole (see Table 1 of Remillard & McClintock 2006, ARA&A 44, 49). Some caution should be applied here though: the maximum mass of NSs is uncertain, and the error bars on the minimum values of M_1 should be carefully examined (1σ, 2σ ...).

The X-ray luminosities of the binaries, $L_X \leq 10^{38}$erg/s, provide an additional clue to the nature of the system. The thermal luminosity of a NS heated to keV temperature would be

$$L_X = 4\pi R^2 \sigma T^4 = 10^{37} R_6^2 T_{\rm keV}^4 {\rm erg/s}, \tag{176}$$

consistent with the observed luminosities. Note also that the lunminosities do not exceed the Eddington luminosity, eq. (23), for a solar mass object.

5.4.3 Double NSs

Rare (7 systems), provide best measurements of masses, plus GR tests. 6 systems with 1 pulsar, 1 system (PSR J0737-3039) a double pulsar. The velocity(ies) is(are) determined from the variations in the pulse(s). The

6 system parameters $\{m, M, a, e, i, \phi\}$ (see § 3.1) are determined from the observed velocity(ies) ($\{e, \phi\}$ from functional form, mass ratio from velocity ratio, total mass from period and velocity up to $\sin i$) and GR effects: the relativistic periastron advance, $\dot{\omega}$, the orbital decay due to gravitational wave damping, $\dot{P}_b$, and the gravitational redshift and time dilation parameter, γ. Thus, the system may be over-constrained (both for single and double pulsars), providing both accurate mass determinations (see fig 6) and tests of GR (actually- of the post-Keplerian parameters, which are measured to satisfy GR relations).

5.5 SNRs: Non thermal emission, collisionless shocks, and cosmic-rays (CRs)

SNRs are observed to emit non-thermal radiation: $\nu L_\nu \propto \nu^{0.5}$ from radio to X-rays, interpreted as synchrotron emission of relativistic electrons with energy distribution $dn_e/dp_e \propto p_e^{-2}$ reaching $cp_e \sim 100$ TeV ($\hbar\omega_{\rm syn} = \hbar\gamma_e^2 eB/m_e c = 1\gamma_{e,8}^2 B_{-5}$ keV where $\gamma_{e,8} = p_e/10^8 m_e c$ and $B = 10^{-5} B_{-5}$G), and high energy emission at TeV energies, interpreted as inverse-Compton scattering of CMB photons by the same high energy electrons ($\gamma_e^2 h\nu_{\rm CMB} = 10\gamma_{e,8}^2$ TeV). The power-law energy distribution of the electrons extending to energies far exceeding the thermal SNR energy of ~ 10 keV, is inconsistent with the exponential distribution, $\propto \exp(-E_e/T)$, expected for a plasma in thermal equilibrium.

5.5.1 Collisionless shocks

The mean free path (mfp) for Coulomb collisions under the conditions of interest, $n_0 \sim 1$ and $T \sim 1$ keV, may be estimated as follows. A strong deflection of a proton by another proton requires passage at a distance $d \sim e^2/T$ so that the mfp is

$$l \sim \frac{1}{n\pi d^2} \sim \frac{T^2}{\pi n e^4} = 10^{19} \frac{T_{\rm keV}^2}{n_0} {\rm cm}. \tag{177}$$

This length scale is larger than (or comparable to) the SNR size. This implies that Coulomb collisions can not provide the scattering mechanism that randomizes the particles' velocities, converting part of their kinetic energy to thermal energy, in the shock transition layer.

In the absence of a scattering process, the fast ejecta plasma would "fly" through the ISM plasma. However, such a situation, where the particle velocity distribution is highly anisotropic (considering both the ejecta and ISM

particle populations), collective plasma instabilities would develop. Electromagnetic and electrostatic plasma waves, related to collective (macroscopic) particle motions, develop at a rate comparable to the plasma frequency, $\omega_{p,i} = \sqrt{4\pi n e^2/m_i}$, leading to isotropization of the velocity distribution. The characteristic length scale of the waves is the plasma skin depth, $c/\omega_{p,i}$. For scattering of protons, that carry most of the momentum and energy,

$$c/\omega_{p,p} = \sqrt{4\pi n e^2/m_p} = 3 \times 10^7 n_0^{-1/2} \mathrm{cm}. \quad (178)$$

We therefore expect a "collisionless shock", for which Coulomb collisions may be ignored, to develop, with a shock transition layer of thickness $\sim c/\omega_{p,p}$. Since Coulomb collisions are not important, they also do not bring the particles to thermal equilibrium past the shock. In the collisional shock case the post-shock plasma is in thermal equilibrium, and its properties are completely determined by the shock jump conditions, independent of the details of the physics within the shock transition layer. In the collisionless case, the post shock plasma is not thermal, and its properties depend upon the details of the processes operating within the transition layer. For this reason, the structure of collisionless shocks and the properties of the post shock plasma are still an open problem. Numerical plasma simulations indicate that collisionless shocks do form, with a transition layer of $\sim 10c/\omega_p$.

Observations and numerical simulations suggest that the energy density of EM waves within the plasma transition region is close to "equipartition", i.e. comparable to the kinetic energy density, $B^2/8\pi \sim \rho_1 v_1^2$. For such a field, the Larmor radius of an incoming proton is $R_L = m_p v_1 c/eB \sim c/\omega_{p,p}$. Thus, "thermal" protons are scattered on a skin depth scale provided the field is close to equipartition.

5.5.2 Particle acceleration

Let us assume that some process "up-scatters" some particles to energy much larger than thermal, $\gg m_p v_1^2$. Such particles will have $R_L \gg c/\omega_{p,p}$, and will therefore cross the shock transition unaffected. Let us further assume that magnetic field irregularities carried by the flow scatter these particles as they propagate through the plasma both in the upstream (ahead of the shock) and in the downstream (past the shock). In this case, the particles may be scattered several times across the shock, before "escaping" to the far downstream (we assume that they never escape to the far upstream, since in an infinite system they will always be scattered back into the shock).

Consider a relativistic particle crossing the shock several times. Let us choose the flow velocity to be negative in the x-direction (i.e. $v = -v_1$ at

$x > 0$, $v = -v_2$ at $x < 0$). We assume that the particles do not change their energy when deflected within the up- or down-stream flows. In this case, each time a particle crosses from down to upstream and back its energy is increased by a factor of $\sim (1 + \Delta v/c)$ where $\Delta v = v_1 - v_2$. This is due to the fact that a particle of energy E measured in the downstream frame has a Doppler boosted energy $(1 + \cos\theta \Delta v/c)E$ in the upstream frame, where θ is the angle between the particle momentum and (the positive direction) x. Since crossing from down to upstream requires $\cos\theta > 0$, the particle energy is larger in the upstream frame. Similarly, for particles crossing from up to downstream, the energy is larger by a factor $(1 + |\cos\theta|\Delta v/c)E$ (the factors are larger than 1 in both cases since both in the up and downstream an observer moving with the plasma sees the plasma at the other side of the discontinuity as approaching him).

Let us consider therefore a system in which a relativistic particle of initial energy E_0 undergoes scattering, such that (i) Its energy after scattering is $(1 + f)$ times its energy prior to scattering, where f is a random variable with distribution independent of the particle energy and $\bar{f} \ll 1$, and that (ii) Between two collisions the particle has an energy independent escape probability $P_{\rm esc}$. What is the probability distribution of the energy with which the particle leaves the system? The energy after the k-th scattering is $E_k = \prod_{i=1}^{k}(1 + f_i)E_0$, so that $\ln(E_k/E_0) = \sum_{i=1}^{k} \ln(1 + f_i)$. For $E_k/E_0 \gg 1$ we must have $k \gg 1$ (since $\bar{f} \ll 1$). For large k, the distribution of $\ln(E_k/E_0)$ would be normal with average $k\overline{\ln(1 + f)} \approx k\bar{f}$ and variance of $\approx k\sigma_f^2$ where σ_f^2 is the variance of f. Thus, for $k \gg 1$ we have a narrow distribution of E_k/E_0, centered around $E_k/E_0 = \exp(k\bar{f})$. The probability for k or more collisions prior to escape is $(1-P_{\rm esc})^k$, so that the probability for escape with energy $> E$ is $P(> E) = (1 - P_{\rm esc})^{\ln(E/E_0)/\bar{f}} = (E/E_0)^{\ln(1-P_{\rm esc})/\bar{f}}$, which in the limit of $P_{\rm esc} \ll 1$ is $P(> E) = (E/E_0)^{-P_{\rm esc}/\bar{f}}$. Thus, the differential energy distribution of escaping particles is

$$\frac{dN}{dE} \propto \left(\frac{E}{E_0}\right)^{-1-P_{\rm esc}/\bar{f}} . \tag{179}$$

Let us calculate next $\bar{f}$ and $P_{\rm esc}$ for the collisionless shock scattering case. Consider the spatial and angular distribution of particles of fixed energy E. This distribution is determined by solving the transport equation of the particles, taking into account the scattering. As we will see below, for non relativistic shocks, $v_1/c \ll 1$, the particle distribution is nearly isotropic in the plasma frame. In this case, particle transport may be approximately described as diffusion, with diffusion coefficient $D = \lambda c/3$, where λ is mfp

(recall the discussion of photon diffusion in stars). Conservation of particles reads

$$\partial_t n + \nabla \mathbf{j} = 0, \quad \mathbf{j} = n\mathbf{v} - D\nabla n, \tag{180}$$

where n is the particle density and j is the flux. For our case, this eq. reduces to

$$v\partial_x n = \partial_x (D\partial_x n). \tag{181}$$

This eq. holds separately for $x < 0$ and $x > 0$, and n should be continuous at $x = 0$ (we assume the shock to be infinitesimally narrow compared to the particles' Larmor radius). This eq. has two solutions,

$$n = n_0, \quad n = n_0 \exp[\int_0^x dx' v/D(x')]. \tag{182}$$

Recalling that $v < 0$ and requiring $n(x = +\infty) = 0$, we must have

$$n = n_0 \begin{cases} 1, & x < 0; \\ \exp[-v_1 \int_0^x dx'/D(x')], & x > 0. \end{cases} \tag{183}$$

The distribution decays in the upstream on a scale $L = D/v_1 \sim \lambda c/v_1$, so that $L/\lambda \sim c/v_1$. Thus, for $v_1 \ll c$ we have $L/\lambda \gg 1$ which ensure isotropy. For relativistic shocks the distribution is highly anisotropic, the diffusion approximation is not valid, and the solution is more complicated.

$P_{\rm esc}$ is obtained from comparing the flux of particles escaping at $x = -\infty$ to the flux of particles crossing the shock into the downstream at $x = 0$,

$$P_{\rm esc} = \frac{-j(-\infty)}{j_-(0)} = \frac{n_0 v_2}{-\int_0^{2\pi} d\phi \int_{\pi/2}^{\pi} d\theta \sin\theta \frac{n_0}{4\pi} c \cos\theta} = \frac{4v_2}{c}. \tag{184}$$

$\bar{f}$ is obtained by considering the average Doppler boost of the particle's energy in crossing from down to upstream and back. For crossing from down to upstream we have

$$\overline{E'/E} = \frac{\int_0^{\pi/2} d\theta \sin\theta \cos\theta (1 + \Delta\beta \cos\theta)}{\int_0^{\pi/2} d\theta \sin\theta \cos\theta} = 1 + \frac{2}{3}\Delta\beta, \tag{185}$$

where $\Delta\beta = (v_1 - v_2)/c$. Since the boost for up to downstream crossing is the same, we have

$$\bar{f} = \frac{4}{3}\frac{v_1 - v_2}{c}, \tag{186}$$

and

$$\frac{P_{\rm esc}}{\bar{f}} = \frac{3}{(v_1/v_2) - 1}. \tag{187}$$

The resulting particle distribution, eq. (179) is therefore independent of the details of the scattering process, depends only on the shock jump conditions. For a strong shock in an ideal gas with $\gamma = 5/3$ we have $P_{\rm esc}/\bar{f} = 1$ and $dN/dE \propto E^{-2}$. This is consistent with the electron spectrum required to explain the SNR non-thermal emission, as well as the non-thermal emission in many high energy astrophysical sources, and also the CR spectrum in the Galaxy (see below). Hence, it is believed that collisionless shock acceleration is responsible for the generation of high energy particles in a wide variety of environments.

Two points are important to emphasize here. First, we have not specified the process that produces particles with initial energy $E_0 \gg m_p v_1^2$. This process is not understood. This is commonly known as the "injection problem". Without understanding the injection we cannot, for example, determine the amount of energy deposited in the accelerated particles. Second, we have treated the accelerated particles as test particles that do not affect the flow. If the energy carried by the accelerated particles constitutes a significant fraction of ρv_1^2, which is indicated by observations, this assumption would break.

Finally, let us consider the maximum energy that may be reached. The particle distribution decays ahead of the shock with a length scale $L(E) = c\lambda(E)/v_1$. Assuming that λ grows with E, then for a system of a finite size, R, the maximum energy reached is determined by $L(E_{\rm max}) \sim R$. Since particles are deflected by magnetic fields, we must have $\lambda > R_L = E/eB$, so that $E_{\rm max} < (v_1/c)BR$.

For SNRs with B comparable to the equipartition field, $B \propto v_1$, we have $v_1 BR \propto v_1^2 R = \dot{R}^2 R$ growing with R as long as the ejecta does not decelerate, and decreasing with R during deceleration. Thus, the maximum energy is achieved at the deceleration radius, given by eq. (166). At and below the deceleration radius the equipartition field is

$$B_{\rm ep} = \sqrt{4\pi\rho_0 v^2} = 5 \left(\frac{n_0 E_{51}}{M/M_\odot} \right)^{1/2} {\rm mG}. \tag{188}$$

This gives, at the deceleration radius

$$E_{\rm max} < 10^{17} \frac{n_0^{1/6} E_{51}}{(M/M_\odot)^{2/3}} {\rm eV}. \tag{189}$$

If the magnetic field ahead of the shock is not amplified by the plasma instabilities to near equipartition, and the accelerated particles are deflected by the magnetic field which exists in the far upstream, $\sim 5\mu$G as typically

found in the ISM, then the maximum energy would be much smaller, $\sim 10^{14}$ eV. Either way, this is sufficient to account for the highest energy electrons inferred to exist, $\gamma_{e,8} \sim 1$ corresponding to 100 TeV.

5.5.3 Galactic cosmic-rays

The ISM is filled with relativistic protons, with energy density $\sim 1\mathrm{eV/cm}^3$ and spectrum $dN/dE \propto E^{-2.7}$ (The ISM also contains a smaller number of relativistic heavy nuclei like C, O, and electrons). The energy density of these "cosmic rays" (CRs) is comparable to that of the ISM magnetic field. This is probably not a coincidence- the CRs are confined to the Galaxy by the ISM magnetic field, and if their energy density becomes higher than that of the field they would escape. The energy density is also similar to the turbulent energy density in the ISM, with characteristic velocity of $\sim 30\mathrm{km/s}$ (and density $\sim 1/\mathrm{cm}^3$). This is probably also not a coincidence, since the ISM magnetic field is probably amplified by the turbulence.

The observations of CRs allows us to infer that the higher energy protons escape the Galaxy faster, with confinement time $\tau \propto E^{-0.5\pm0.1}$. This implies that the CRs are generated with a spectrum $d\dot{N}/dE \propto E^{-2.2}$ (since $dN/dE = \tau d\dot{N}/dE$). This is consistent with the spectrum expected from collisionless shock acceleration discussed above. Given the estimates of the confinement time and the energy density of CRs, it is estimated that CRs should be produced in the Galaxy at a rate of $\sim 10^{40}\mathrm{erg/s} = 10^{49.5}\mathrm{erg}/100$ yr. Since the SN rate in the Galaxy is estimated as $\sim 1/100$ yr, the observed Galactic CRs may be produced by SNe if they deposit $\sim 1\%$ of their energy in CRs. It is thus commonly believed that the Galactic CR protons (and heavier nuclei) with energies reaching at least ~ 1000 TeV are produced by SNRs (see eq. 189).